REGISTRATION OF TERRESTRIAL LASER SCANNER DATA USING IMAGERY

Khalil Al-Manasir, Ph.D student
Clive S. Fraser, Professor
Department of Geomatics
University of Melbourne
Victoria 3010
Australia
k.al-manasir@pgrad.unimelb.edu.au
c.fraser@unimelb.edu.au

ABSTRACT

Building 3D models using terrestrial laser scanner (TLS) data is currently an active area of research, especially in the fields of heritage recording and site documentation. Multiple TLS scans are often required to generate an occlusion-free 3D model in situations where the object to be recorded has a complex geometry. The first task associated with building 3D models from laser scanner data in such cases is to transform the data from the scanner's local coordinate system into a uniform Cartesian reference datum, which requires sufficient overlap between the scans. Many TLS systems are now supplied with an SLR-type digital camera, such that the scene to be scanned can also be photographed. The provision of overlapping imagery offers an alternative, photogrammetric means to achieve point cloud registration between adjacent scans. The images from the digital camera mounted on top of the laser scanner are used to first relatively orient the network of images, and then to transfer this orientation to the TLS stations to provide exterior orientation. The proposed approach, called the IBR method for Image-Based Registration, offers a one-step registration of the point clouds from each scanner position. In the case of multiple scans, exterior orientation is simultaneously determined for all TLS stations by bundle adjustment. This paper outlines the IBR method and discusses test results obtained with the approach. It will be shown that the photogrammetric orientation process for TLS point cloud registration is efficient and accurate, and offers a viable alternative to other approaches, such as the well-known iterative closest point algorithm.

INTRODUCTION

The first requirement of 3D modeling an object or scene via terrestrial laser scanning (TLS) is to transform the overlapping point clouds from adjacent scans into a uniform Cartesian reference coordinate system. One of the popular approaches adopted for this registration process is the Iterative Closest Point (ICP) algorithm for surface matching developed by Besl & MacKay (1992). Several variations of the ICP algorithm have been formulated (Chen & Medioni, 1992; Zhang, 1994; Masuda & Yokoya, 1995; Bergevin et al., 1996), including the use of sensor acquisition geometry to search for point correspondences, as proposed by Park & Subbarao (2003). Also, an initial solution for a subsequent application of the ICP method using the normal distribution transform (NDT) has been reported by Ripperda & Brenner (2005), while Gruen & Akca (2005) have suggested the Least Squares 3D Surface Matching (LS3D) method. For a review of current 3D surface registration algorithms the reader is referred to Campbell & Flynn, (2001) and Gruen & Akca (2005).

Terrestrial laser scanner manufacturers generally supply an SLR-type digital camera with the laser scanner to facilitate generation of photo-realistic 3D virtual models. In this paper, a point cloud registration method is described, which makes use of the imagery accompanying the TLS point cloud to determine scanner exterior orientation and thus scan-to-scan registration. The digital camera is first photogrammetrically calibrated via a self-calibration process, after which it is mounted on the scanner. The camera's exterior orientation with respect to the TLS reference coordinate system is then determined, again photogrammetrically. Subsequently, the photogrammetric orientation of imagery from a digital camera mounted on the TLS is performed via relative orientation or bundle adjustment in order to transform all the scanned data into a common coordinate system.

OVERVIEW OF THE REGISTRATION METHOD

A Nikon D100 6-megapixel digital camera with an 18mm lens is shown rigidly mounted on a Riegl LMS-Z210 TLS in Fig. 1. If the exterior orientation parameters of the camera coordinate system *(x,y,z)* with respect to the laser coordinate system *(X,Y,Z)* are known, then the relative orientation between overlapping images from two stations recorded with the metrically calibrated camera can also provide the transformation parameters required to co-register the two accompanying laser point clouds.

Figure 1. The Nikon D100 camera rigidly attached to the Riegl TLS.

Following a self-calibration stage, the camera position with respect to the laser scanner coordinate system need only be recovered once. TLS and image data from two or more stations are then recorded, with there being a requirement for image overlap, but not necessarily overlap between the TLS point clouds. A photogrammetric orientation for the two or more overlapping images provides the exterior orientation parameters for the camera stations with respect to a single reference coordinate system. By also knowing the camera position within the TLS coordinate system, the registration of point clouds is directly established. A primary motivation for this image-based registration (IBR) process is avoidance of the often problematic process of identifying conjugate points within the laser scan data.

THE MATHEMATICAL MODEL

3D Coordinate Transformation

The mathematical relationship between two overlapping TLS point clouds can be simply expressed as a 3D similarity transformation:

$$\begin{pmatrix} X_1 \\ Y_1 \\ Z_1 \end{pmatrix} = \lambda \mathbf{R} \begin{pmatrix} X_2 - X^c \\ Y_2 - Y^c \\ Z_2 - Z^c \end{pmatrix} \tag{1}$$

where (X_1, Y_1, Z_1) and (X_2, Y_2, Z_2) represent Scan 1 and Scan 2 coordinates; **R** a rotation matrix, which is formed from three axial rotation angles here termed ω, φ and κ; and (X^c, Y^c, Z^c) the translation components between Scan 1 and Scan 2. Since the laser range data establishes absolute scale, the applicable scale factor λ has unit value, so Eq. 1 represents a rigid body transformation. Once the six transformation parameters (scale is assumed fixed) are computed between the point clouds, the XYZ coordinates of all scan points can be transformed into a common coordinate system.

Camera Calibration

The photogrammetric registration approach initially involves a one-off camera calibration via an independent self-calibration network. With the use of appropriate coded targets and software, the image measurement and computation of calibration parameters is a fully automatic process, as described for example in Cronk et al. (2006). The software system used for this stage of the project was *Australis* (Fraser & Edmundson, 2000; Photometrix,

2006). The automation aspect is of importance for camera calibration because it is wise to periodically re-check the camera interior orientation parameters. The calibration model is that of the extended collinearity equations, with eight additional parameters:

$$x - x_0 + \Delta x = -c\frac{R_1}{R_3}$$
$$y - y_0 + \Delta y = -c\frac{R_2}{R_3} \qquad (2)$$

where

$$\begin{pmatrix} R_1 \\ R_2 \\ R_3 \end{pmatrix} = \mathbf{R} \begin{pmatrix} X - X^c \\ Y - Y^c \\ Z - Z^c \end{pmatrix}$$

and

$$\Delta x = -x_0 - \frac{\bar{x}}{c}\Delta c + \bar{x}r^2K_1 + \bar{x}r^4K_2 + \bar{x}r^6K_3 + (2\bar{x}^2 + r^2)P_1 + 2P_2\bar{x}\bar{y}$$
$$\Delta y = -y_0 - \frac{\bar{y}}{c}\Delta c + \bar{y}r^2K_1 + \bar{y}r^4K_2 + \bar{y}r^6K_3 + 2P_1\bar{x}\bar{y} + (2\bar{y}^2 + r^2)P_2 \qquad (3)$$

Here, *(x,y)* are image coordinates, *x* and *y* departures from collinearity; *c* a correction to the principal distance *c*; x_0 and y_0 the principal point coordinates; *X,Y,Z* object point coordinates; X^c, Y^c and Z^c translations; K_i the coefficients of radial lens distortion and P_i those of decentring distortion. This physical additional parameter model is currently preferred for digital camera self-calibration (eg Fraser, 1997). For practical reasons, the camera is removed from the TLS for self-calibration, since camera roll is precluded while it is mounted, yet roll angle diversity is critical for an accurate recovery of interior orientation parameters.

Camera to TLS Orientation

Following the calibration phase, the camera is again mounted on the TLS at a fixed alignment, as in Fig. 1, and an image and a scan are recorded. This one-off operation allows the position and orientation of the camera with respect to the TLS coordinate system to be determined using spatial resection. The mathematical model for spatial resection is the well-known formulation based on the collinearity equations. It is effectively that of Eq. 2 with *(x,y)* constituting the observations, and the parameters of exterior orientation (the three rotation angles forming **R** and X^c, Y^c and Z^c) being the unknowns. Initial starting values for the least-squares solution of the resection problem are determined by a closed-form algorithm similar to that of Quan & Lan (1999) and Zeng & Wang (1992). The 'control points' used, which should number 10 or more well spread points for accuracy and reliability, are selected from the TLS scan data.

Relative Orientation of Images

Within the TLS survey, two or more scans are recorded, such that the images from the TLS stations sufficiently overlap to support a photogrammetric relative orientation or bundle adjustment. The well-known coplanarity model (eg Mikhail et al., 2001) has been adopted to solve the relative orientation of an image pair, since approximated object space coordinates are not required for a solution. The coplanarity model can be formulated from the perspective projection represented by Eq. 2, for the case of one image being relatively oriented to a second, as:

$$\mathbf{u}_1^{\mathrm{T}} \begin{pmatrix} 0 & bz & -by \\ -bz & 0 & bx \\ by & -bx & 0 \end{pmatrix} \mathbf{R}_2^{\mathrm{T}} \mathbf{u}_2 = 0 \qquad (4)$$

where

$$u_i = \begin{pmatrix} x' & y' & -c \end{pmatrix}_i^T$$

Here, *(x',y')* represent image coordinates refined and corrected for principal point offset and lens distortion, the matrix $\mathbf{R}_2$ describes the rotation of the second image with respect to the first, and *by* and *bz* are translations. The translation *bx*, which lies in the baseline, can be assigned an arbitrary value since scale cannot be recovered from the coplanarity model. Scale is applied to the relatively oriented network using point-to-point distances determined between image identifiable laser scanned points. The coplanarity equations are solved via least-squares, with a minimum of five suitably distributed points being necessary to recover the three rotation angles and two translations, though use of 10 or more corresponding points is recommended.

As in the earlier resection, the determination of initial values in the least-squares solution is critical if the process is to be highly automated. To solve the problem of initial value determination, a Monte Carlo approach described in Cronk et al. (2006) has been adopted. In this approach, the most plausible initial relative orientation solutions are determined, effectively by trial and error. These are then refined by least squares and the correct solution is automatically determined.

In the case of multiple overlapping images and TLS data sets, it is possible to further refine the exterior orientation in a bundle adjustment, though this well known model will not be further described in detail here.

Point Cloud Registration

The mathematical relationship between the camera and TLS coordinate system can be expressed as follows:

$$\begin{pmatrix} x \\ y \\ z \end{pmatrix} = \lambda \mathbf{R}_{\mathrm{C}} \begin{pmatrix} X - X^c \\ Y - Y^c \\ Z - Z^c \end{pmatrix} \tag{5}$$

where *(x, y, z)* represent the camera's coordinate system and *(X, Y, Z)* are the TLS point coordinates. The rotation matrix $\mathbf{R}_C$ expresses the relative alignment between the axes of the two systems and (X^c, Y^c, Z^c) describes the position of the camera with respect to the origin of the TLS coordinate system. In this case the scale factor λ again has unit value. With the relative orientation between two images *i* and *j* determined, the point cloud registration can be established via the transformation established from a combination of Eqs. 4 and 5:

$$\begin{pmatrix} X \\ Y \\ Z \end{pmatrix}_i = \mathbf{R}_{\mathrm{A_i}}^{-1} \cdot \left(\mathbf{R}_C^{-1} \cdot \left[\mathbf{R}_{j,i}^{-1} \cdot \begin{pmatrix} x \\ y \\ z \end{pmatrix}_j + \begin{pmatrix} bx \\ by \\ bz \end{pmatrix} \right] + \begin{pmatrix} X^c \\ Y^c \\ Z^c \end{pmatrix} \right)_j \tag{6}$$

where

$$\begin{pmatrix} x \\ y \\ z \end{pmatrix}_j = \mathbf{R}_{\mathrm{C}} \cdot \left[\mathbf{R}_{\mathrm{A_j}} \cdot \begin{pmatrix} X \\ Y \\ Z \end{pmatrix}_j - \begin{pmatrix} X^c \\ Y^c \\ Z^c \end{pmatrix} \right]$$

and *i* is the reference point cloud with *j* being the data set whose coordinates are to be transformed. The camera position and orientation in the TLS coordinate system at a specific alignment of the scanner, when the rotation angle *A* of the scanner shown in Fig. 2 is zero, are expressed by the 3x3 rotation matrix $\mathbf{R}_C$ and the translation vector (X^c, Y^c, Z^c). The 3x3 rotation matrix $\mathbf{R}_{j,i}$ and the translation vector *(bx, by, bz)* are formed by the exterior orientation of camera station *j* within the reference coordinate system of camera station *i*; and $\mathbf{R}_A$ is a 3x3 rotation matrix defining the TLS rotation around its Z-axis described by the angle *A* at the time of exposure.

EXPERIMENTAL RESULTS

Three experimental applications of the IBR method are now summarized. The first was a 3-scan survey of camera calibration testfield comprising an array of targets of known coordinates, the second involved the 3D

modeling of a cultural heritage site, and the third was selected to illustrate the registration of non-overlapping TLS point clouds using the IBR approach.

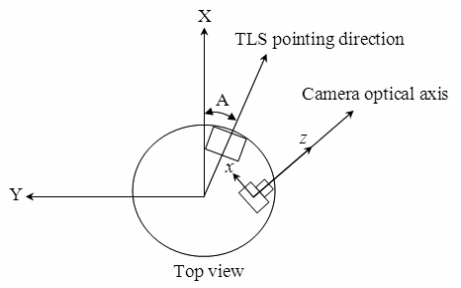

Figure 2. Relationship between the TLS coordinate system and the optical axis of the camera.

Survey of a Calibration Testfield

The first experiment involved the modeling of a target field used for research into sensor calibration in close range photogrammetry. The testfield comprises a mostly planar array of 160 retro-reflective targets, mounted upon both a wall and a section of ceiling, as shown in Fig. 3. This testfield represented an ideal site at which to evaluate the automatic relative orientation and registration of overlapping point clouds. The nine large square targets were used to compute the camera position and orientation within the TLS coordinate system (Eq. 5).

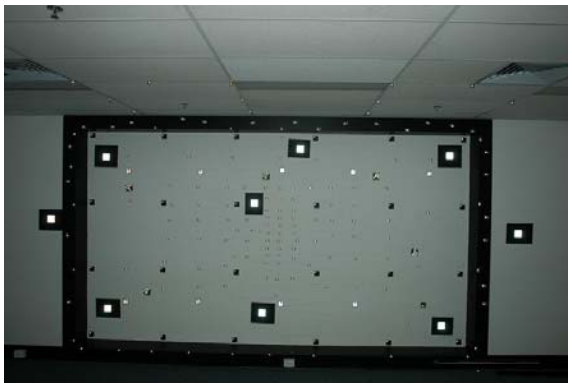

Figure 3. The calibration wall comprised of retro-reflective targets.

A photogrammetric network of 14 convergent images was established to self-calibrate the camera. The images were recorded from a set-back distance of about 4m. The coded targets in Fig. 3 (small squares) were used to facilitate automatic network orientation and self-calibration via the *Australis* software system. The high quality of the calibration is indicated by the low magnitude of the image coordinate residuals, which had an RMS value of 0.05 pixels or 0.4 m. The Nikon D100 was mounted on the Riegl TLS, as per Fig. 1, following the camera calibration.

In the next stage of the process the relationship between the camera and TLS coordinate systems was established. A single scan of the calibration wall was recorded, along with a single image. The centroids of the nine prominent retro-targets seen in Fig. 3 were measured in the image and a spatial resection performed. The resulting accuracy of the camera position and orientation was 0.5mm for position and 10 seconds of arc for the three orientation angles. Given the inherent accuracy of the Riegl scanner, of about 25mm over a 4m distance, the resection result was deemed satisfactory for the subsequent registration and was expected to produce a registration accuracy that would surpass that using TLS scan data alone.

The IBR method was performed to register the three overlapping scans of the calibration wall, as shown in Fig. 4. Firstly, images associated with Scan 3 and 2 were relatively oriented via Eq. 4, using more than 25 automatically extracted image points. After the resection of the image associated with Scan 1, using the 3D object point coordinates which were determined from the relative orientation process of images 2 and 3, a bundle adjustment was performed using all three images.

The transformation of the TLS points in Scans 1 and 2 into Scan 3 was performed using Eq. 6, thus completing the registration process. Because the retro-targets could be identified by their intensity characteristics, it was possible to compare the final XYZ coordinates to known values which had previously been determined in a photogrammetric survey of significantly higher accuracy. The resulting residuals against the 100 check points are shown in Table 1. The 2mm accuracy achieved is viewed as quite acceptable and well within that anticipated for the TLS. A further registration of the three TLS point clouds was created using the ICP method, in which the retro-targets were identified by their intensity values and compared to the known check points. As shown in Table 1, this registration yielded an accuracy of 2.5mm.

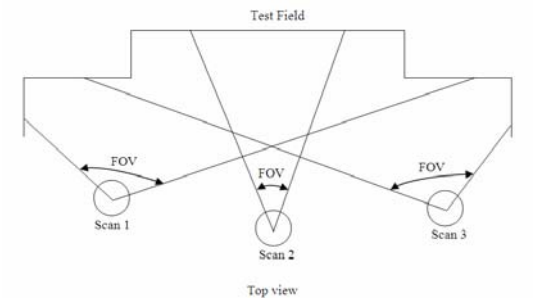

Figure 4. Three-scan coverage of the calibration wall.

Table 1. RMSE of registered point clouds with respect to calibration wall control points.

Registration method	No. of control points	Overall RMSE (mm)
ICP	100	2.5
IBR method	100	2.0

Modeling of Captain Cook's Cottage

The second experiment involved the 3D modeling of Captain Cook's Cottage, a heritage site and popular tourist attraction in Melbourne. The cottage was scanned from seven different stations with the Riegl scanner. The laser data comprised about 3.5 million points. Seven images were recorded with the mounted Nikon D100 camera, one from each TLS station. Sufficient overlap was provided between images so as to ensure robust relative orientation and subsequent bundle adjustment. All images were recorded with the laser scanner pointed in its X-direction so $\mathbf{R}_A = I$ as indicated in Fig. 5.

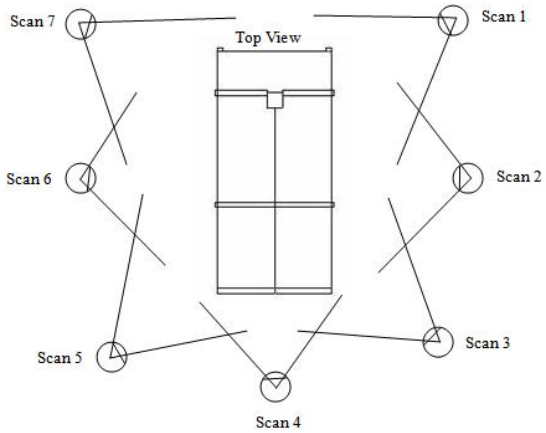

Figure 5. Scanner/camera station geometry for the survey of Cook's cottage.

In the photogrammetric solution, the image in Scan 1 was adopted as the reference scan for the network, and the subsequent bundle adjustment of all seven images was then performed. The image measurements were manual since no special targets were placed on the object.

The images associated with Scan 1 and 2 were first relatively oriented via Eq. 4 using more than 30 manually extracted image points. Care was taken to select points such that at least four, the minimum required for the closed-form spatial resection algorithm, would be identifiable and measurable in the images from the stations Scan 3 though to Scan 7. A bundle adjustment of all images was then performed, which produced an RMS value of image coordinates of 0.5 pixels. The resulting 1-sigma accuracy of the photogrammetrically determined object points was at the 2mm level, ie well within the specified accuracy of the Riegl TLS. Registration of the laser scans was then carried out via Eq. 6, with the resulting, registered 3D point cloud being shown in Fig. 6.

Figure 6. The 3D model of Cooks' cottage from TLS data.

The resulting RMS discrepancy between the model registered via the IBR approach and that of an ICP-generated model was 2.7mm, with the largest residuals being 4mm in the grassed area in front of the cottage (see Fig. 7). A visual analysis of the error map does not suggest the presence of any systematic misalignment between the two 3D models, which indicated that for all practical purposes the two solutions were equivalent.

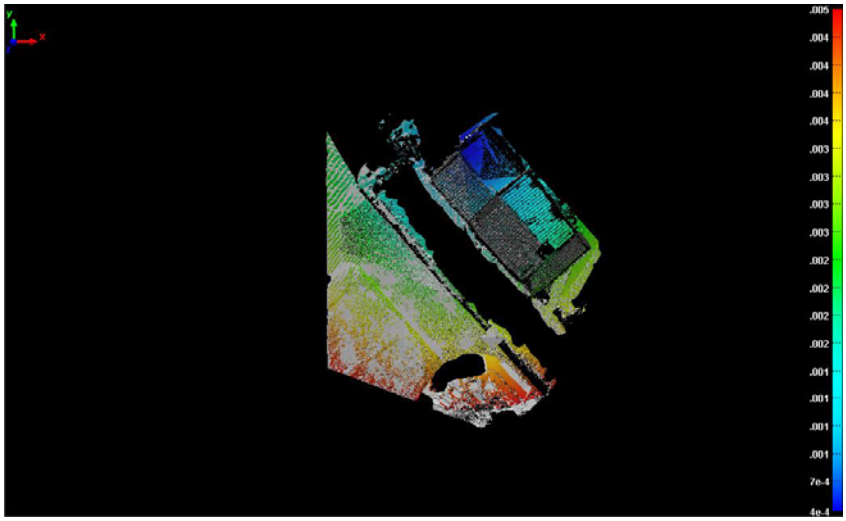

Figure 7. Map of discrepancies between final closest points in the IBR & ICP data sets (units are m).

Modeling a Building Entrance

The third experiment was carried out to demonstrate the ability of the proposed IBR method to register non-overlapping TLS point clouds, as illustrated in Fig. 8. Two scans were recorded with the Riegl scanner, along with two images from the Nikon D100 camera. The camera was pointing to an adjacent building next to the site being scanned. This ensured that there would be sufficient overlap between images to support robust relative orientation and subsequent bundle adjustment – but no overlap between the TLS point clouds. Another two images were recorded (shown as Image 1 and Image 2) using the demounted Nikon D100, in order to improve the strength of the photogrammetric network.

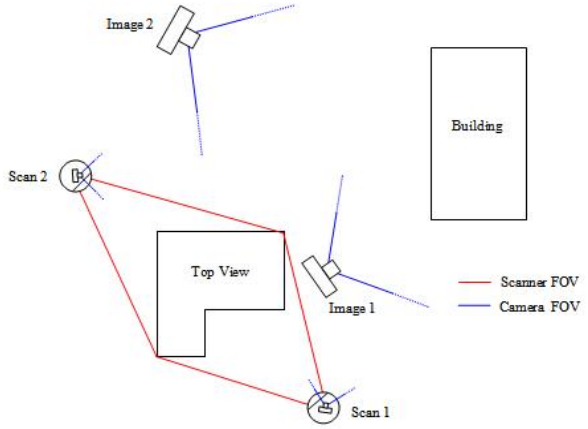

Figure 8. Scanner/camera station geometry highlighting non-overlapping TLS data.

A relative orientation was performed between the images from the stations Scan 1 and Scan 2, followed by a 4-image bundle adjustment which produced an RMS value of image coordinate residuals of 0.4 pixels. The resulting 1-sigma accuracy of the photogrammetrically determined object points was 2mm. Registration of the two laser scans was then carried out via the IBR method (Eq. 6). In order to check the accuracy of the registered 3D point cloud from the IBR approach, nine control points, which had previously been determined in a photogrammetric survey of significantly higher accuracy, were identified manually in the registered 3D point cloud. The resulting absolute RMS point positioning errors from the IBR approach are shown in Table 2, where X & Y are planimetric coordinates.

Table 2: Point positioning errors in the IBR registration.

Number of check points	RMSE X(mm)	RMSE Y(mm)	RMSE Z(mm)
9	4.2	4.5	3.1

CONCLUSIONS

The IBR method for registration of laser scanner data using photogrammetric orientation has been described, and test results from three trial applications of the method have been reported. The IBR method has been shown to provide a practical alternative to current TLS registration approaches such as the ICP algorithm. Moreover, the method is fast compared to the ICP algorithm, and has the prospect of being more accurate, though this aspect needs further confirmation. One benefit of the IBR method is that the selection of conjugate points in digital imagery is generally a more straightforward and less error prone process than the same operation with laser scan data that includes intensity values. The proposed method is robust and does not require any overlap between the separate TLS point clouds. This can be a significant benefit. Also, the IBR approach can overcome known difficulties associated with existing laser scanner registration algorithms and in many instances it can serve as an alternative to the ICP algorithm and LS3D approach. The IBR method can also constitute an initial solution for both the ICP and the LS3D approaches where registration via these algorithms might be more appropriate, for example where it is only possible to form a weak relatively oriented network of images.

REFERENCES

Bergevin, R., Soucy, M., Gagnon, H. and Laurendeau, D. (1996). Towards a general multi-view registration technique. *IEEE Transactions on Pattern Analysis and Machine Intelligence,* 18(5), 540– 547.

Besl, P.J. and McKay, N.D. (1992). A method for registration of 3-D shapes. *IEEE Transactions on Pattern Analysis and Machine Intelligence,* 14(2): 239-256.

Campbell, R.J. and Flynn, P.J. (2001). A survey of free-form object representation and recognition techniques. *Computer Vision and Image Understanding,* 81(2): 166-210.

Chen, Y. and Medioni, G. (1992). Object modelling by registration of multiple range images. *Image and Vision Computing,* 10(3): 145-155.

Cronk, S., Fraser, C.S. and Hanley, H. (2006). Automatic calibration of colour digital cameras. Submitted to *Photogrammetric Record*, 19 pages.

Fraser, C.S. (1997). Digital camera self-calibration. *ISPRS Journal of Photogrammetry and Remote Sensing,* 52(4):149-159.

Fraser, C.S. and Edmundson, K.L. (2000). Design and implementation of a computational processing system for off-line digital close-range photogrammetry. *ISPRS Journal of Photogrammetry and Remote Sensing,* 55(2): 94-104.

Gruen, A. and Akca, D. (2005). Least squares 3D surface and curve matching. *ISPRS Journal of Photogrammetry and Remote Sensing,* 59(3): 151-174.

Masuda, T. and Yokoya, N. (1995). A robust method for registration and segmentation of multiple range images. *Computer Vision and Image Understanding,* 61(3): 295-307.

Mikhail, E.M., Bethel, J.S. and McGlone, J.C. (2001). *Introduction to Modern Photogrammetry*. John Wiley & Sons, New York. 479 pp.

Park, S.Y. and Subbarao, M. (2003). A fast point-to-tangent plane technique for multi-view registration*. IEEE International Conference on 3-D Digital Imaging and Modeling*, Banff, October 6-10, pp. 276-283.

Photometrix (2006). Website for *Australis* system: www.photometrix.com.au, accessed 30 January 2006.

Quan, L. and Lan Z. (1999). Linear N-point camera pose determination. *IEEE Transactions on Pattern Analysis and Machine Intelligence,* 21(8): 774-780.

Ripperda, N. and Brenner, C. (2005). Marker-Free registration of terrestrial laser scans using the normal distribution transform. *ISPRS Workshop on Virtual Reconstruction and Visualization of Complex Architectures*, Mestre-Venice, Italy, August 22-24, on CD-ROM.

Zeng, Z. and X. Wang (1992). A general solution of a closed-form space resection. *Photogrammetric Engineering and Remote Sensing,* 58(3): 327-338.

Zhang, Z. (1994). Iterative point matching for registration of free-form curves and surfaces*. International Journal of Computer Vision,* 13(2):119-152.